



The Dynamics of Aerotaxis in a Simple Eukaryotic Model

Marta Biondo¹, Cristina Panuzzo², Shahzad M. Ali², Salvatore Bozzaro², Matteo Osella¹, Enrico Bracco^{3†} and Barbara Pergolizzi^{2*†}

¹ Department of Physics, INFN, University of Turin, Turin, Italy, ² Department of Clinical and Biological Science, University of Turin, Turin, Italy, ³ Department of Oncology, University of Turin, Turin, Italy

OPEN ACCESS

Edited by:

Robin S. B. Williams,
University of London, United Kingdom

Reviewed by:

Igor Weber,
Rudjer Boskovic Institute, Croatia
Paul Robert Fisher,
La Trobe University, Australia

*Correspondence:

Barbara Pergolizzi
barbara.pergolizzi@unito.it

[†] These authors have contributed
equally to this work and share last
authorship

Specialty section:

This article was submitted to
Molecular and Cellular Pathology,
a section of the journal
Frontiers in Cell and Developmental
Biology

Received: 04 June 2021

Accepted: 13 October 2021

Published: 23 November 2021

Citation:

Biondo M, Panuzzo C, Ali SM,
Bozzaro S, Osella M, Bracco E and
Pergolizzi B (2021) The Dynamics
of Aerotaxis in a Simple Eukaryotic
Model.

Front. Cell Dev. Biol. 9:720623.
doi: 10.3389/fcell.2021.720623

In aerobic organisms, oxygen is essential for efficient energy production, and it acts as the last acceptor of the mitochondrial electron transport chain and as regulator of gene expression. However, excessive oxygen can lead to production of deleterious reactive oxygen species. Therefore, the directed migration of single cells or cell clumps from hypoxic areas toward a region of optimal oxygen concentration, named aerotaxis, can be considered an adaptive mechanism that plays a major role in biological and pathological processes. One relevant example is the development of O₂ gradients when tumors grow beyond their vascular supply, leading frequently to metastasis. In higher eukaryotic organisms, aerotaxis has only recently begun to be explored, but genetically amenable model organisms suitable to dissect this process remain an unmet need. In this regard, we sought to assess whether *Dictyostelium* cells, which are an established model for chemotaxis and other motility processes, could sense oxygen gradients and move directionally in their response. By assessing different physical parameters, our findings indicate that both growing and starving *Dictyostelium* cells under hypoxic conditions migrate directionally toward regions of higher O₂ concentration. This migration is characterized by a specific pattern of cell arrangement. A thickened circular front of high cell density (*corona*) forms in the cell cluster and persistently moves following the oxygen gradient. Cells in the colony center, where hypoxia is more severe, are less motile and display a rounded shape. Aggregation-competent cells forming streams by chemotaxis, when confined under hypoxic conditions, undergo stream or aggregate fragmentation, giving rise to multiple small loose aggregates that coordinately move toward regions of higher O₂ concentration. By testing a panel of mutants defective in chemotactic signaling, and a catalase-deficient strain, we found that the latter and the *pkbR1^{null}* exhibited altered migration patterns. Our results suggest that in *Dictyostelium*, like in mammalian cells, an intracellular accumulation of hydrogen peroxide favors the migration toward optimal oxygen concentration. Furthermore, differently from chemotaxis, this oxygen-driven migration is a G protein-independent process.

Keywords: aerotaxis, oxidative stress, hydrogen peroxide, collective cell migration, *Dictyostelium*, G-protein, catalase

INTRODUCTION

Oxygen (O₂) is required for cell survival, oxidative metabolism, and synthesis of adenosine 5'-triphosphate (ATP), being the final electron acceptor in oxidative phosphorylation (Wilson, 2017). Moreover, advances in the understanding of the physiology of O₂ have shown that it is also important as a signaling molecule. Indeed, in multicellular organisms, it is an essential micro-environmental factor controlling developmental processes (Dunwoodie, 2009).

Maintenance of cellular O₂ level, supply, and consumption are precisely regulated, as oxygen imbalance could increase reactive oxygen species (ROS) production. To maintain oxygen homeostasis, metazoan organisms use the hypoxic signaling pathway to facilitate O₂ delivery and cellular adaptation to oxygen deprivation (Claesson-Welsh, 2020). Mammalian cells under hypoxic conditions adapt rather quickly by inhibiting proliferation and relying on glycolysis rather than oxidative phosphorylation for energy production, thus preventing further O₂ consumption. As a consequence, all these processes increase the production of angiogenic factors that can drive vascular remodeling and eventually improve tissue perfusion and O₂ delivery (Rey and Semenza, 2010).

The relationship between O₂ depletion and cancer is a common feature among most solid tumors. The hypoxic core microenvironment provides an aggressive ecological selective pressure for resilient stem-like cancerous cells. Furthermore, hypoxic environmental conditions may induce advanced and dysfunctional vascularization and promote epithelial-to-mesenchymal transition, resulting in high cell mobility and a high risk of developing metastasis (Muz et al., 2015). In this regard, O₂ gradients are crucial in early stages of sarcoma development, where cells respond to the hypoxic gradient by aggressively invading the matrix, and subsequently show fast and long-distance migration (Lewis et al., 2016). Furthermore, immortalized mammary epithelial cells, residing within deep hypoxia, migrate directionally toward oxygen by the process named aerotaxis, through an ROS-dependent enhanced epidermal growth factor receptor (EGFR) activation (Deygas et al., 2018).

Although the reports described above suggest that O₂ acts as a chemoattractant for cancer cells to the neighboring blood vessels, the molecular players and signaling pathways triggering this process remain understudied. Aerotaxis has been long studied in prokaryotes (Taylor et al., 1999; Sporer et al., 2017), whereas in eukaryotes it started to be investigated in *Caenorhabditis elegans* (Gray et al., 2004; Chang et al., 2006; Demir et al., 2020), the choanoflagellate *Salpingoeca rosetta* (Kirkegaard et al., 2016), and more recently in mammalian cells (Deygas et al., 2018). In all these cases, cells can first sense and navigate toward oxygen and then react appropriately by eventually organizing a coordinated and directional movement. Nonetheless, the molecular players remain largely unknown.

A relevant part of current knowledge of the mechanisms regulating oriented cell migration, in response to various stimuli, has been obtained in the social amoeba *Dictyostelium discoideum*, which has proven to be an excellent model system to study almost every kind of random and directional cell motility, including chemo-, electro-, and rheo-taxis (Bozzaro, 2013; Lima et al., 2014; Devreotes and Horwitz, 2015; Jeon et al., 2019; Guido et al., 2020). Cell motility is very similar in *Dictyostelium* and neutrophils, and the molecular components involved in cell migration are remarkably conserved between *Dictyostelium* and mammalian cells (Stuelten et al., 2018; Bozzaro, 2019; Pal et al., 2019).

Based on this large plethora of studies and the availability of well-defined mutants in genes regulating cell motility and signal transduction (Fey et al., 2019), we thought that *Dictyostelium* could be a very suitable model for studying aerotaxis. In this report, we analyzed aerotactic migration parameters in *Dictyostelium* wild-type cells and a panel of mutants defective in chemotaxis and/or electrotaxis. In agreement with previous findings in mammals, the oxygen sensing of *Dictyostelium* cells seems very likely associated with high cytoplasmic levels of hydrogen peroxidase. Furthermore, the observed "aerotaxis" does not share the signaling pathways regulating chemotaxis and electrotaxis.

MATERIALS AND METHODS

Dictyostelium discoideum Cell Culture and Development

The parental wild-type (WT) AX2 and mutant strains were cultured in an axenic medium (Ashworth and Watts, 1970) at 23°C under shaking at 150 rpm as previously described (Pergolizzi et al., 2017b). The mutant strains were obtained from the Dicty Stock Center¹, except for mutant HSB1, available in the laboratory, generated by chemical mutagenesis as described (Bozzaro et al., 1987), and previously characterized as temperature-sensitive for the *piaA* gene (Pergolizzi et al., 2002).

Aerotaxis Assay

The aerotaxis assay was modified from Deygas et al. (2018). Basically, growing *Dictyostelium* cells were seeded at a density of approximately 10,000 cells/mm² as a 10-μl drop containing 50,000 cells in the center of a 24-well culture plate. After cell attachment to the substratum, 400 μl of the axenic medium was added, and two 14 mm-diameter glass coverslips were placed on top to cover and confine the cell cluster. As a control in the not-confined (NC) system condition, cells were simply seeded without coverslips.

To assay the ability of aggregation competent cells to sense oxygen gradients, axenically growing AX2 cells were washed twice in a Soerensen phosphate buffer and resuspended at 5 × 10⁶ cells/ml. Afterward, a 10-μl drop containing 50,000

¹www.dictybase.org

cells was spotted in the center of the 24-well culture plate and let adhere for 10 min, before covering with 400 μl of buffer. The cells were then confined immediately (t_0) or after 7 h (t_7) when the aggregates were well-formed. No confinement (NC) conditions were used as a control of the experiment.

Time lapse movies of cell migration under confinement (C) or no confinement (NC) were recorded with times up to 24 h using a Lumenera Infinity 3 camera coupled to a Zeiss Axiovert 200 microscope, with a $5\times$ objective. Photograms were taken at intervals varying between 20 and 360 s (Pergolizzi et al., 2017b).

Quantification of Cell Arrangement During Migration

In our experimental setting, the circular 10- μl *Dictyostelium* cell layer was approximated to a bidimensional system of cells adhering to the substrate.

Therefore, the cell density (i.e., number of cells per unit area) represents a convenient parameter to characterize and define the arrangement of cells within the cluster. To quantitatively measure the density of cells, bright field images were split into portions of a defined and regular area, and the number of cells was determined using the Python package Trackpy (Allan et al., 2021).

Alternatively, in case of high cellular density, a much simpler indirect cell density measurement approach was undertaken represented by the relative number of cells expressed as percentage (%). Briefly, the bright field images were binarized through an adaptive threshold using the Python library OpenCV (Bradski, 2000). As a result, the cells appeared as white shapes on a black background in the binarized images. Brightness, i.e., the fraction of white pixels, can be used to detect changes in cell density as a first approximation. By partitioning the binarized images in circular areas, this method has been used to draw the cell density heat maps and radial profiles of the relative number of cells at different times. The latter were then analyzed to measure the displacement of its peak, which identifies the *corona*.

To investigate the role of cell duplication during collective migration, we instead considered a circular sector of the cell cluster and we segmented single cells using Trackpy (Allan et al., 2021). The increase in the number of cells counted in this specific area can only be attributed to cell duplication, since for symmetry reasons we do not expect on average any net flux of cells through the sector.

Analysis of the “Corona” Features

The most visually striking peculiarity of the migration pattern of the confined *Dictyostelium* cells consisted in the formation of a ring of high cell density, which we named *corona*, that moves away from the hypoxic region.

To characterize the kinetics and pattern features of this process, we first measured the formation time of the *corona* (T^*), defined as the time required to detect a local maximum in the cell distribution profile at the periphery of the cell cluster.

Measuring the distance between the peak of cellular density and the center of the colony identified the position of the ring. Next, we determined the kinetics of the ring displacement $\Delta R(t)$

(R = radius; t = time) by assessing either its average velocity during the first 2 h after its formation (v_i) or for longer time points (v_f) (i.e., 10–24 h). T^* , v_i , and the propagation of the ring have been quantified in at least three experiments for each cellular strain.

The features of the ring dynamics (i.e., width and density in time) were assessed in three independent experiments in the period 10–24 h by setting a minimum threshold value for the cell density. We acquired one measurement every 6 min and performed data binning to group five measurements per data point (data point \pm vertical bar = mean value \pm standard deviation).

Estimation of the Expansion Velocity of the Non-confined Cell Cluster

To describe the spreading of the cell cluster in the absence of cell confinement, we analyzed the first 5 h of independent experiments in the non-confined conditions. For each experiment (exp), we located the border of the cluster setting a minimum threshold value (t_h) for the density profiles; we assessed the displacement of the cluster border to measure the instantaneous expansion velocity of the cluster over 1-min time-lapse [$^{exp}v_{t_h}(t)$], and we then averaged these values to determine the spreading velocity $^{exp}v_{t_h}$. Since the choice of the cell density threshold was arbitrary, we considered a range of possible values, obtaining a set of $^{exp}v_{t_h}$ that was averaged to estimate the expansion velocity of the cluster (^{exp}v). We repeated this evaluation process for three independent experiments, and we measured $v_{NC} = 0.8 \pm 0.3 \mu\text{m}/\text{min}$ (mean value \pm standard deviation) that can be used as reference value for further comparisons with the cell dynamics in confined conditions.

Single Cell Tracking

Employing the Trackpy package, we determined the aerotactic pattern of *Dictyostelium* cells from the point of view of single cells: for both the confined and not confined conditions, we analyzed a video lasting 30 min with a resolution of three frames per minute providing the tracking software with the parameters “typical size” and “maximum speed” of the cells (10 μm and 10 $\mu\text{m}/\text{min}$, respectively). Given the symmetry of the colony, single-cell trajectories were described using polar coordinates (R, θ). The instantaneous speed [$|v|(t_i, R)$], radial component of the velocity [$v_r(t_i, R)$], and ratio between them [$v_r/|v|(t_i, R)$] were measured over time periods of 1 min for each detected cell. These measurements were grouped according to their distance from the center of the colony (R) using the sliding window method (150 μm interval) to describe the average motility of cells in a given position [$\langle |v| \rangle (R)$, $\langle v_r \rangle (R)$, and $\langle v_r/|v| \rangle (R)$].

Cell tracking was also performed on videos of cells uniformly distributed over a plate to quantify their spontaneous motility in the absence of any hypoxia condition or oxygen gradient.

Oxygen Level Measurement

Oxygen concentration was determined over time using the VisiSens detector unit DUO1 coupled to the oxygen sensor foil SF-RPSu4. Data were analyzed with the AnalytiCal1 software

(PreSens, Germany). Under our experimental conditions, the time lapse of cell displacement and oxygen level detection were two mutually exclusive measurements.

RESULTS

Dictyostelium Cells Migrate and Regularly Deploy in Response to an Oxygen Gradient

We sought to assess whether *Dictyostelium* cells were able to sense an oxygen gradient and to move directionally toward the oxygen source. To generate an O₂ gradient, we took benefit of the method previously developed by Deygas et al. (2018) and modified it as indicated in the section “Materials and Methods.” The oxygen gradient was induced by confining (C) the cells under coverslips. As a control, not confined (NC) cells were used. Oxygen levels were directly visualized by dynamic measurements with the VisiSens detector unit, confirming the different hypoxic profiles between the two conditions (Supplementary Figure 1).

A detailed analysis revealed that growing *Dictyostelium* cells moved with a peculiar pattern toward the higher oxygen concentration when subjected to confinement conditions. After approximately 1 h, a fraction of confined cells began to move coordinately, assuming an arrangement characterized by a thickened front, the *corona*, that once shaped, persistently moved toward the oxygen source (Figure 1A and Supplementary Movie 1). Interestingly, underneath the *corona*, the cells lined up in two further regimes that were easily recognized because of their differential cell density (Figure 1B). At the center of the colony, where oxygen concentration was lowest (Supplementary Figure 1), the cells were rather rounded, and their density was highest, although on average it decreases by 35% in the time-range 10–24 h. This stratification of the cluster in three density regimes was found to be fairly constant over time. The central area abutted with a wide region with lowest cellular density, in which the cells displayed an elongated shape (Figure 1B). While the size of the central high-density region was approximately constant, the lowest density sector expanded as the ring moved away from the center. Interestingly, the cells that trigger the formation of the *corona* were not the outermost ones (Supplementary Figure 2 and Supplementary Movies 1, 2).

The shape of the cell clusters in C or NC was very similar at the beginning of the experiment (Figure 2A), displaying a circular geometry with the cell density decreasing as it approached the periphery (Figure 2B). Noticeably, in the NC system, cell distribution was maintained throughout the time. The only difference detected was the progressive spreading of the cell cluster with typical velocity of the cluster expansion $v_{NC} = 0.8 \pm 0.3 \mu\text{m}/\text{min}$, presumably by virtue of random cell motility and cell duplication, as the cells are incubated in a nutrient-rich growth medium.

On the contrary, under confined (C) conditions, we noticed that the pattern of cell arrangement was considerably dynamic over time. When compared with the onset condition, a thickened circular front, the *corona*, featured by a relatively high cell density,

emerged, and persistently moved radially following the same direction of the oxygen gradient (Figure 2B).

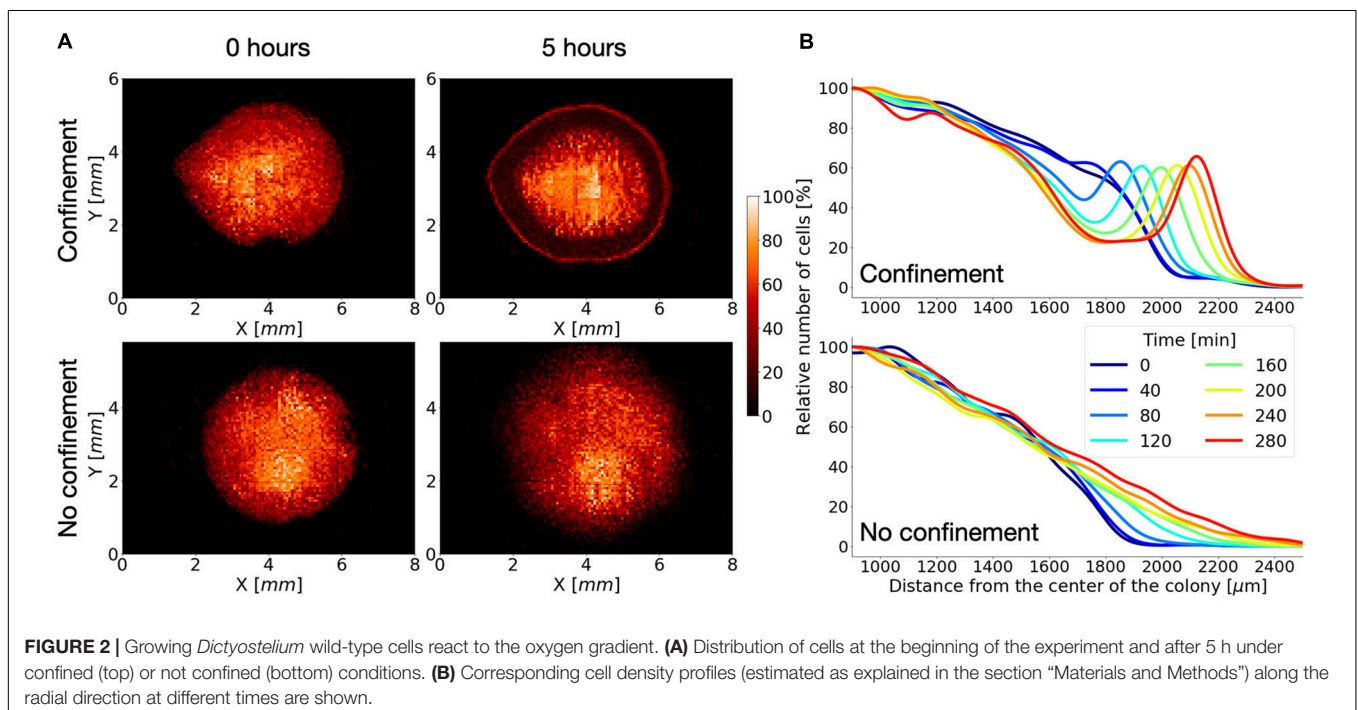
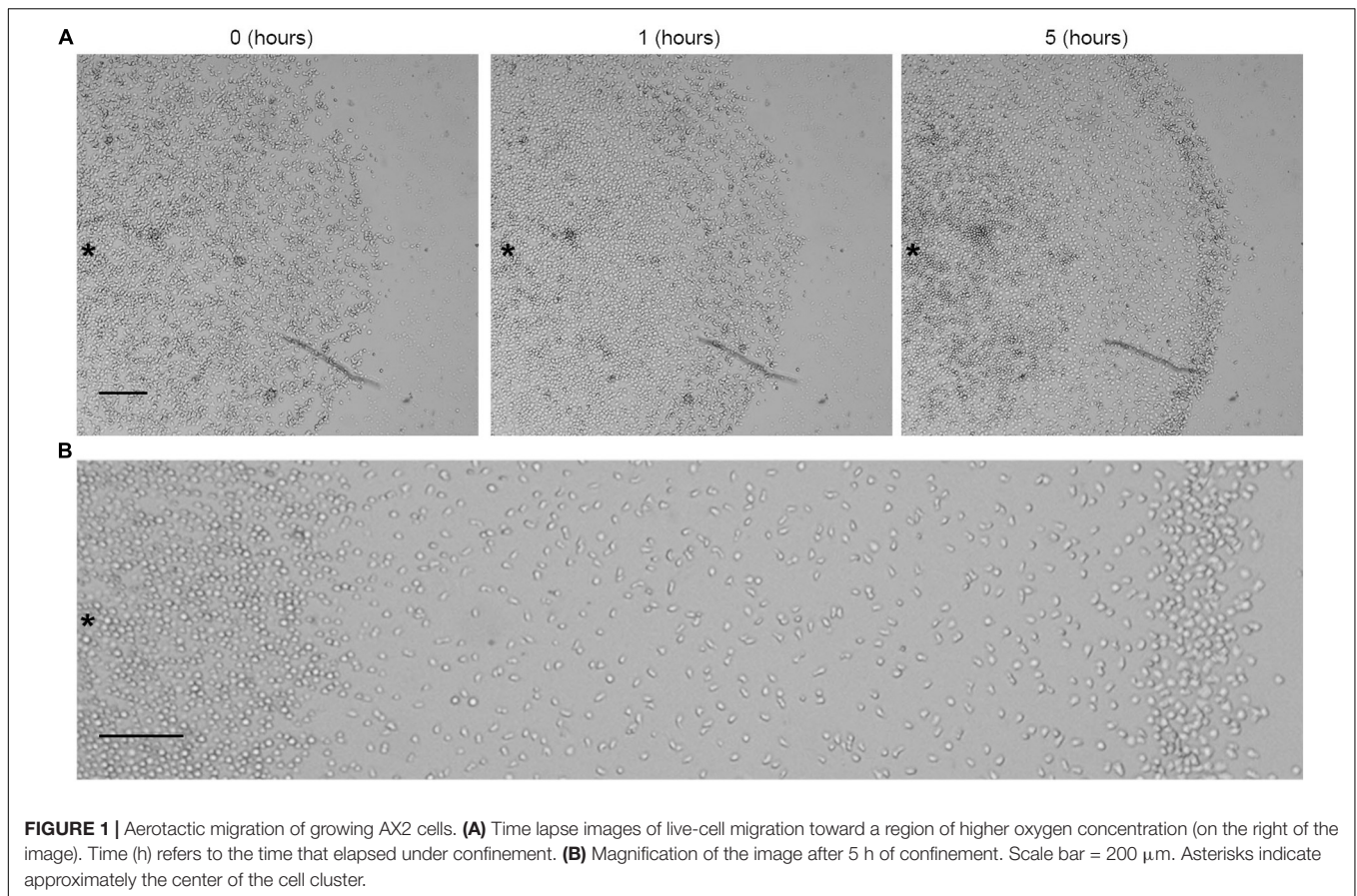
To exclude that what we observed was the outcome of the pressure caused by the glass coverslips, we also performed the NC experiment by adding an amount of the axenic medium corresponding to the weight of the glass coverslips (0.1 g). Even under such conditions, the cells displayed a behavior identical to that of the NC counterpart (data not shown), indicating that the outcome observed under confinement was tightly associated with hypoxic stress.

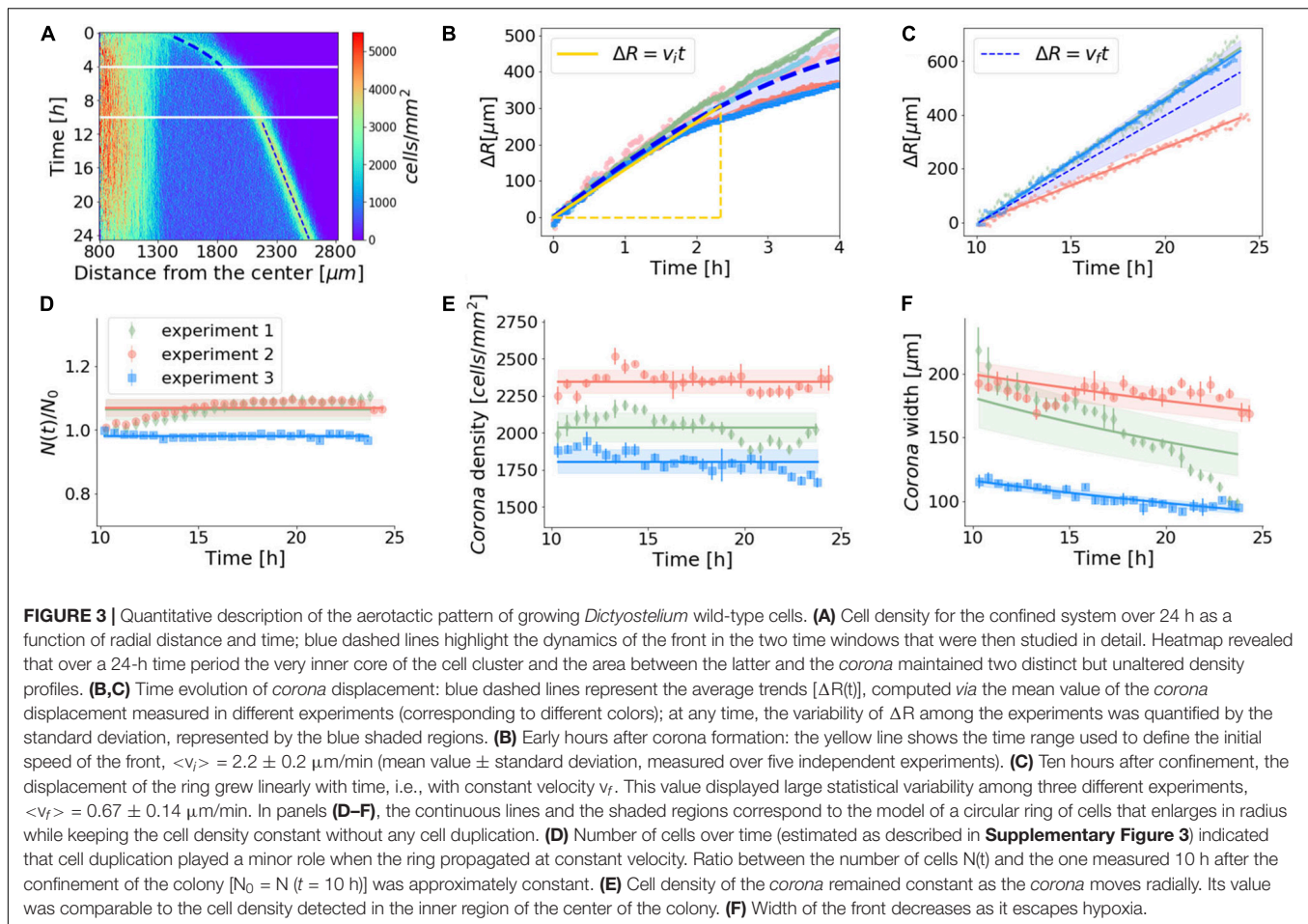
Assessment of the Dynamic Physical Properties of the *corona* Structure

We then examined the peculiar biological process by which the vegetative *Dictyostelium* cell cluster reacted to the confined system within 24 h. Using density profiles, we determined the time required for the *corona* formation under confinement (T^*), which turned out to be nearly 60 ± 20 min for the parental strain AX2 (Supplementary Table 1). Concerning the dynamics of the *corona*, besides experimental variability, we found that after a transient period of a few hours, the initial velocity (v_i) of the *corona* propagation decreased until it reached a constant value (v_f), after approximately 10 h (Figure 3A). The initial velocity (v_i) of the *corona*, measured within the first 140 min, was equal to $2.2 \mu\text{m}/\text{min}$ (Figure 3B), but then it fell sharply to approximately 30% of v_i ($v_f = 0.67 \mu\text{m}/\text{min}$) and remained constant for the rest of the experiment, i.e., in the time range 10–24 h (Figure 3C). The decline in the *corona* speed is not sudden but rather smooth. This non-linear velocity trend could simply reflect continuous changes in microenvironmental conditions (e.g., variations of the oxygen profile in the radial direction). Our experimental settings (i.e., cells in the axenic medium and a 24-h time window) are, in principle, compatible with cell proliferation. Indeed, our estimates of cell duplication (Supplementary Figure 3 for details) revealed that, under confinement, the cells were growing within the first few hours, but that after 10 h the number of cells in the colony was essentially constant (Figure 3D). At least within the 10–24 h period, cell growth can be regarded as a negligible effect and, thus, scarcely impacts the *corona* dynamics.

We then assessed the *corona* cell density in the time range 10–24 h. Despite experimental fluctuations, our measurements indicate that, on average, after 10 h, the *corona* cell density reached a steady state (Figure 3E).

If the number of cells that compose the *corona* and coordinately migrate is constant, as suggested by the fact that cell duplication is negligible, in order to maintain the same cell density, the width of the *corona* has to decrease. These simple geometric arguments provide an analytic prediction given the circular shape of the *corona* and the empirical linear growth in time of the *corona* radius $R(t) = R_0 + \Delta R(t)$. If a *corona* of width $L(t)$ and radius $R(t)$ has to conserve the total area of the ring, its width will decrease as $L(t + \Delta t) = L(t)R(t)/R(t + \Delta t)$. The parameters of this model are the average number of cells $[N(t)]$, the cell density within the *corona*, and its area. For each



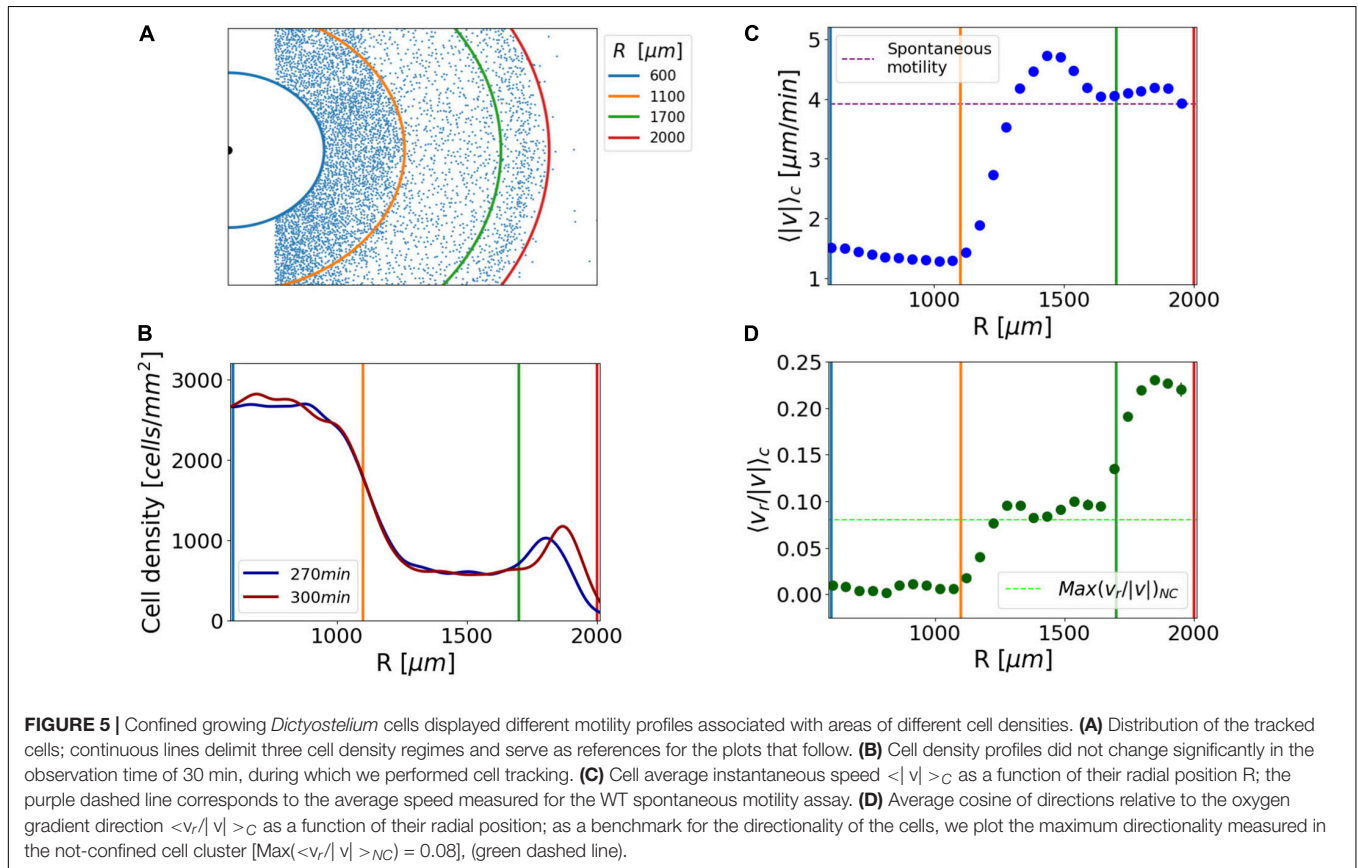
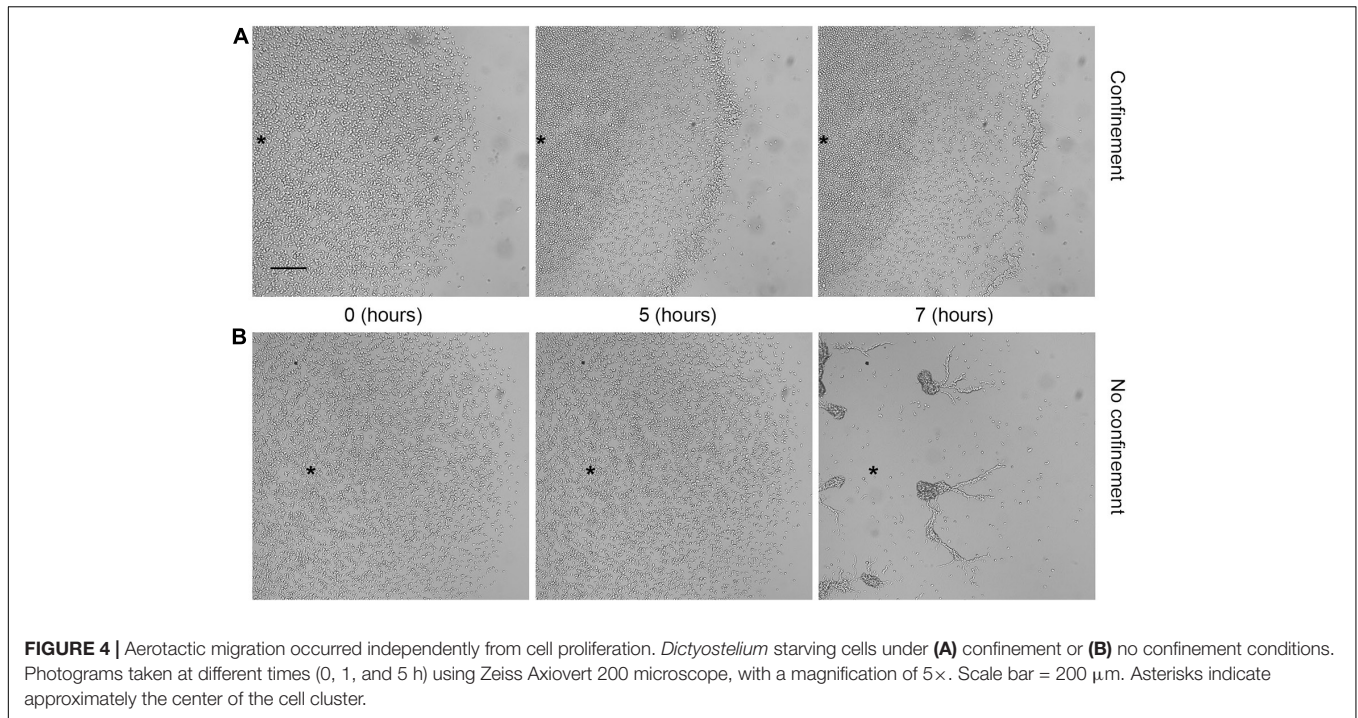


experiment (represented in **Figures 3C–F** by different colors), we independently estimated the best values of these parameters and their error (mean \pm standard deviation), and used them to produce respectively the continuous lines and the shaded regions in **Figures 3D–F**, which can explain reasonably well the empirical trends that we observed. To further exclude a role of cell duplication in the formation and progression of the *corona*, we assayed aerotaxis in starving WT cells, which are unable to duplicate. Even under these conditions, the cellular behavior was indistinguishable from that of growing cells (**Figure 4** and **Supplementary Movie 3**). As expected, under starvation, the cells lying within the *corona* reached the aggregation competence with timing comparable with that of the unconfined cells. Indeed, a *corona*-like front emerges within 2 h and persists for up to 4–5 h. By this time, the starving cells become aggregation-competent and start aggregating by chemotaxis driven by self-generated cAMP. This leads to fragmentation of the *corona* in streaming aggregates. These results confirm that cell division plays a negligible role in the formation of the *corona*. In addition, this assay proves that the exhaustion of nutrients does not represent a key event in triggering the movement toward the oxygen source, because otherwise the *corona* formation of starving cells would be faster than the response of growing cells. Ultimately, these findings also suggest that the *corona* structure represents a barrier

to the oxygen to flow in the inner core of the cluster and when fragmented, because cells aggregate, and the oxygen gradient becomes discontinuous, thus inhibiting the formation of a new *corona*.

Different Motility Features Are Associated With the Cluster Density Profiles

We examined single-cell tracks of the confined cluster to ascertain cell motility features, such as average directionality, speed, and their association with the distance from the center. A survey was carried out in three different regions, namely, the center of the cell cluster, the *corona*, and the region in between (**Figure 5A**). The analysis was performed over 30 min in the time frame between 270 and 300 min, which was a convenient time scale to track thousands of cells per frame without significant changes in the cell cluster density profile and in the *corona* displacement (**Figure 5B**). To quantify the single cell motility, we measured the average instantaneous speed [$\langle |v| \rangle_c$], at different distances from the cluster center. Conversely, the cell directionality was examined, by determining the average ratio between the radial component of the instantaneous velocity and the instantaneous



speed [$\langle v_r/|v| \rangle_C$]. To assess the average directionality of cells in the absence of a substantial oxygen gradient, we tracked the cells of the not confined system during the same timeframe.

Our analysis identified three different motility profiles, strictly associated with the three regions of different cellular density previously described. On average, cells lying in the center of the cluster ($600 \mu\text{m} < R < 1,100 \mu\text{m}$) displayed a rather stationary behavior with minor or no displacement (**Figure 5C**). Notably, those fewer cells showing displacement did not exhibit any preferential direction with respect to the geometry of the system [$\langle v_r/|v| \rangle_C = 0$].

The cells embedded in the *corona* ($R > 1,700 \mu\text{m}$) displayed an average instantaneous speed comparable with that of cellular random motility ($3.9 \mu\text{m}/\text{min}$, **Figure 5C**). For the sake of clarity, we refer to random motility as that recorded for growing cells seeded under no confinement and incubated in the axenic medium. The comparison between the average $\langle v_r/|v| \rangle_C$ of the cells belonging to the *corona* and the directionality measured in the non-confined cell cluster $\langle v_r/|v| \rangle_{NC}$ allowed us to conclude that the former exhibited evident directionality toward regions of higher oxygen concentration. As a matter of fact, the value of $\langle v_r/|v| \rangle_{NC}$ calculated as a function of the distance from the center had a maximum value of 0.08 in the outer colony region. On the other hand, $\langle v_r/|v| \rangle_C$ is 0.24 if evaluated in the *corona* returned to 0.08 in the low-density region (**Figure 5D**). In order to support this result, we performed a Von Mises fit of cell angular displacement distributions to estimate the mean direction (μ) and the accuracy of the orientation (k) of the cells of the *corona* (Fisher and Annesley, 2006). Given the initial cell distribution within the cluster and the circular symmetry of the system, it was not surprising that the mean direction of cells was the radial one. However, we next imposed $\mu = 0$, and assessed the accuracy of the orientation (k). The directionality of the cells belonging to the *corona* was higher than the one measured for the confined cells in the intermediate region and for cells in the not confined cluster (**Supplementary Figure 4A**).

When compared with the very inner region of the cell cluster, cells in the intermediate low-density region, ($1,100 \mu\text{m} < R < 1,700 \mu\text{m}$) showed higher speed with a velocity peak immediately behind the *corona* (**Figure 5C**).

In conclusion, cells in the intermediate region displayed an appreciable movement directionality toward the oxygen source $\langle v_r/|v| \rangle_C > 0$ (**Figure 5D**), but compatible with the random spreading of *Dictyostelium* from a high cell density region as measured in the not-confined system [$\langle v_r/|v| \rangle_C \approx \text{Max}(\langle v_r/|v| \rangle_{NC})$]. Similarly, the average radial velocity of the cells in the low-density region was compatible with the rate of expansion of the non-confined cluster $\langle v_r \rangle_C \approx v_{NC}$ (**Supplementary Figures 4B,C**) suggesting again that the migration in this area could not be driven by the oxygen gradient.

The reduced directionality of the cells of the intermediate region with respect to those belonging to the *corona* implies that it is unlikely that cells of the intermediate region can supply the *corona*. Therefore, it is likely that the cells that

migrate coordinately in the *corona* are always the same (i.e., their number is conserved).

Hypoxia Selectively Blocks *Dictyostelium* Cell Aggregation and Triggers Oxygen-Dependent Collective Migration

When starved under normoxic conditions (18–21% O_2), *Dictyostelium* cells aggregate, generate migratory slugs, and ultimately culminate to form fruiting bodies. Oxygen concentration regulates the aggregate size and the orientation of the prestalk-prespore pattern (Sternfeld and Bonner, 1977; Sternfeld and David, 1981), while below 10%, oxygen hinders culmination (Sandona et al., 1995). To test the ability of aggregation-competent cells to react to hypoxia, we assessed aerotaxis in cells starved for 7 h. Briefly, aggregates formed under submerged conditions were confined and then assayed. Within the first few minutes, the aggregates suffered profound rearrangements, getting looser and partially disaggregating. Eventually, within the next 30–40 min, the loose aggregates directionally moved following the oxygen gradient (**Supplementary Movie 4**). Single cells still exhibited their elongated shape and arranged themselves in streaming-like structures (**Figure 6A**) that eventually moved toward the oxygen source displaying collective cell migration. Under such conditions, the absence of a clear-cut *corona* can be a consequence that the aggregates give rise to a discontinuous hypoxic gradient all over the cell cluster.

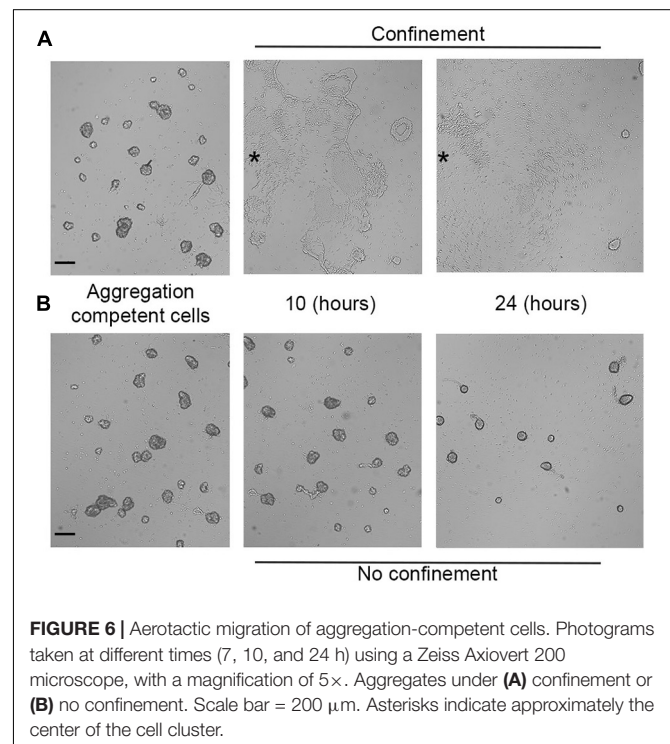


FIGURE 6 | Aerotactic migration of aggregation-competent cells. Photographs taken at different times (7, 10, and 24 h) using a Zeiss Axiocvert 200 microscope, with a magnification of 5 \times . Aggregates under **(A)** confinement or **(B)** no confinement. Scale bar = 200 μm . Asterisks indicate approximately the center of the cell cluster.

In the NC control, the aggregates became more compact as time progressed (Figure 6B).

Dictyostelium Aerotactic Migration Relies on Impaired Intracellular Hydrogen Peroxide Degradation but Not on Chemotaxis Signaling Pathways

In mammalian cells migration toward an oxygen gradient is associated with a significant accumulation of H₂O₂ at the border of the cell cluster. This represents the most prominent event coinciding with the onset of directional motility (Deygas et al., 2018).

Based on this finding, we sought to assess the aerotaxis process in a *Dictyostelium* mutant defective in catalase activity (Garcia et al., 2002). This enzyme catalyzes the decomposition of H₂O₂ into H₂O and O₂. As a consequence, mutants with no catalase activity are hypersensitive to oxidative stress from hydrogen peroxide. Indeed, *catA*^{null} cells display a severely impaired response to hydrogen peroxide even at a very low concentration (Supplementary Figure 5).

The aerotactic migration of the *catA*^{null} mutant was assayed and compared with that of the WT. With regard to the cell density profiles, they were indistinguishable. On the contrary, the kinetics of the process highlighted that the time required to organize the *corona* (T*) was shortened for *catA*^{null} when compared with that of the WT cells (Figure 7A). The *catA*^{null} showed a decline of T* of approximately 50% (28 ± 2) (Figure 7D and Supplementary Table 1). In contrast, the initial velocity (v_i) of the *corona* propagation of *catA*^{null} cells exhibited only a moderate increase when compared with that of the WT (Figure 7E and Supplementary Table 1). Therefore, although evolutionarily distant, both *Dictyostelium* and mammalian cells utilize intracellular H₂O₂ as an activator or enhancer of aerotactic migration.

We also tested a panel of mutants defective in chemotaxis and/or electrotaxis to assess whether they displayed altered aerotaxis, suggesting potential links between these motility processes. As summarized in Supplementary Table 2, the mutants either fail to aggregate at all or display impaired aggregation because of defects in the signaling pathways. A preliminary qualitative analysis of all the mutants showed that none of the strains displayed major defects in aerotaxis.

Quantitative analysis was restricted to three mutants: the Gβ^{null} mutant, which lacks the beta subunit of the G protein and is, thus, essential for transducing GPCR chemotactic signals (Lilly et al., 1993; Pergolizzi et al., 2017a); the HSB1 mutant, harboring the *pianissimo* gene mutation *pia*^{G917D}, required for adenylyl cyclase activation (Pergolizzi et al., 2002); and *pkbR1*^{null} (Meili et al., 2000), defective in the PKB/AKT related kinase. Under confinement, all the mutants behave as the WT cells (Figures 7B,C and Supplementary Figure 6). With the only exception of the *pkbR1*^{null} strain, in which a moderate decline in the time required for *corona* formation (T*) was observed, for the other mutants, no significant differences were detected (Figure 7D and Supplementary Table 1). However, the *pkbR1*^{null} and, to a much lesser extent, Gβ^{null} strains exhibited higher initial

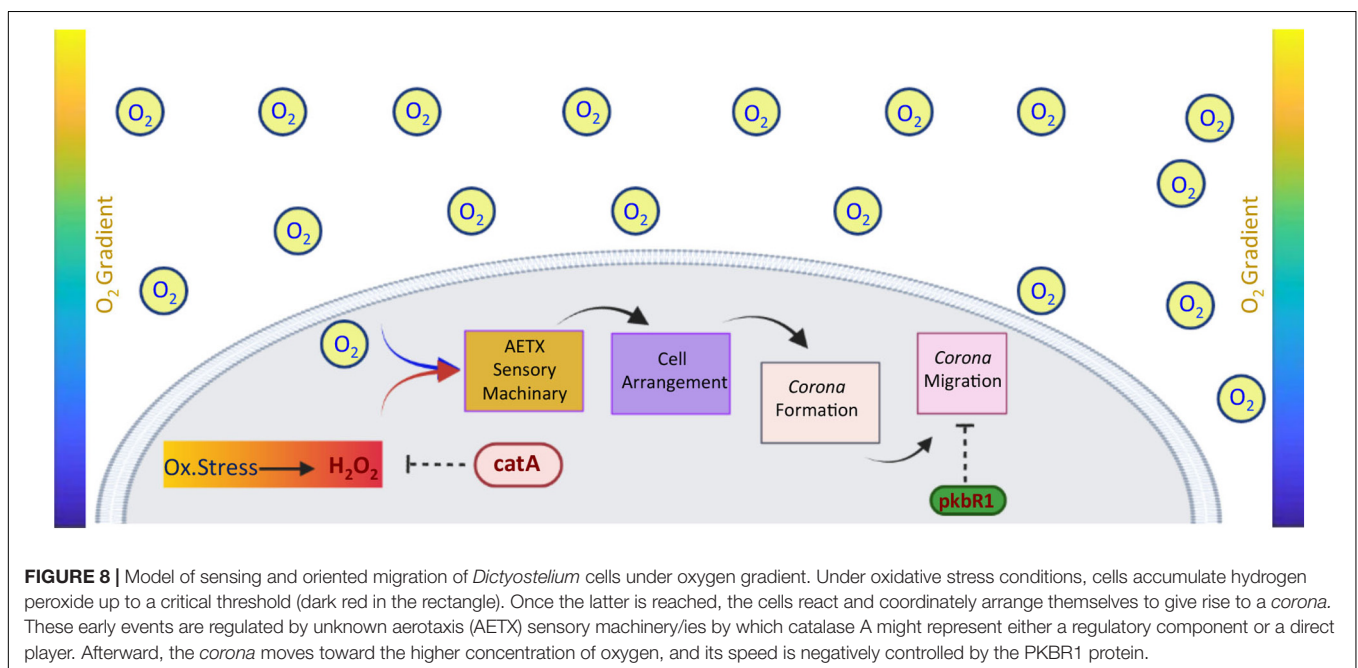
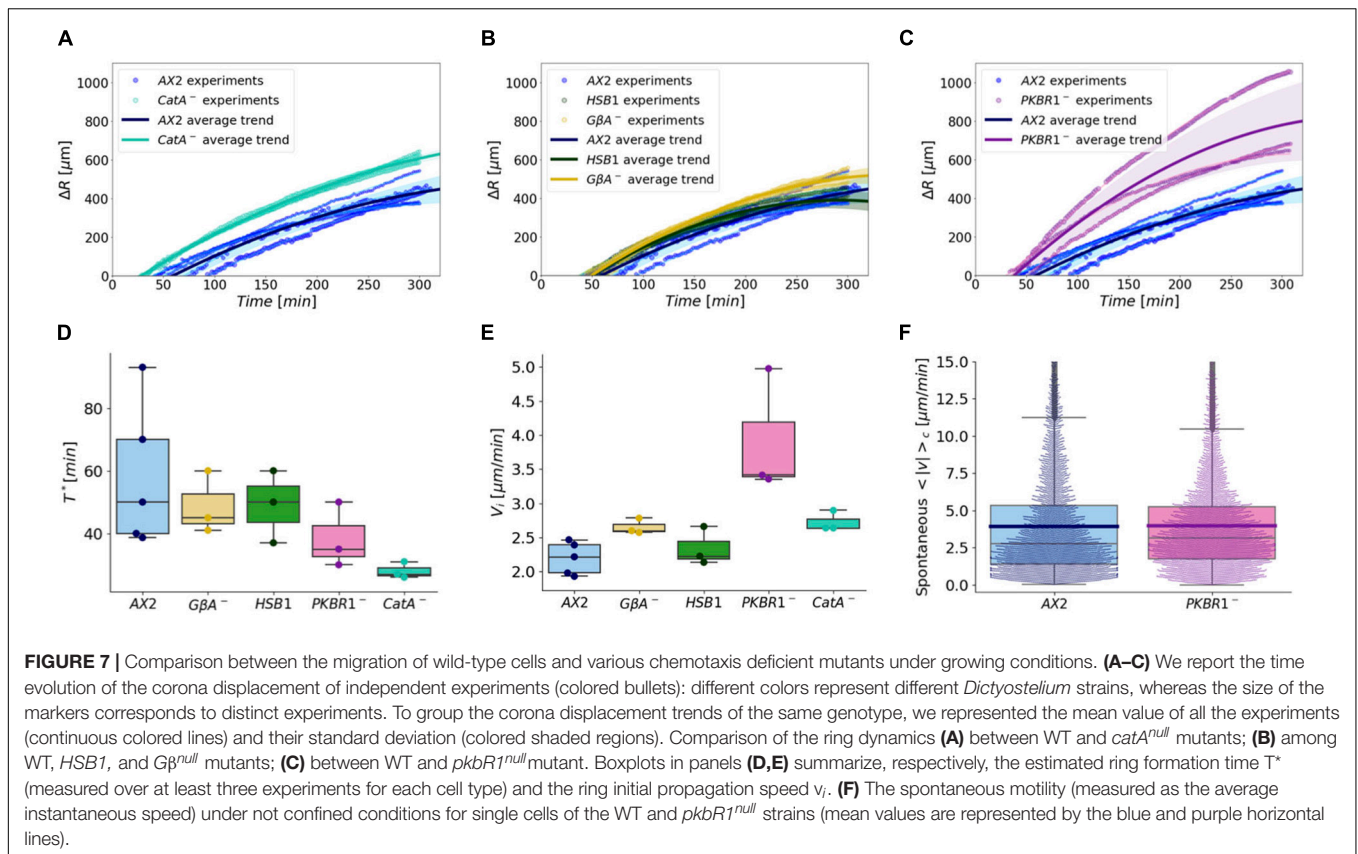
propagation speed of the *corona*, and the latter similar to *catA*^{null} (Figure 7E and Supplementary Table 1). These results suggest that signals transduced via G-protein coupled receptor(s) and PKBR1 serve to restrain or inhibit the sensitivity of the cells to O₂ gradients in aerotaxis. Conversely, such differences were abolished when considering the time scale of within 10–24 h (Supplementary Figure 7). To rule out that the prominent initial speed detected in *pkbR1*^{null} cells was the outcome of increased single cell motility, we also measured its spontaneous motility and compared it with that of the WT. We found that the random movement of *pkbR1*^{null} cells displayed an average speed basically indistinguishable from that of the WT strain AX2 (Figure 7F).

DISCUSSION

Mild to severe O₂ deprivation (hypoxia) due to high tumor cell metabolic rate and aberrant vascularization is associated with altered cellular metabolism as well as resistance to chemotherapy and radiotherapy (Horsman and Overgaard, 2016; Parks et al., 2017). Furthermore, hypoxia regulates cell proliferation and supports apoptosis evasion by tumor cells. On the whole, hypoxia exerts a selection pressure that leads to the survival of subpopulations of viable cells with the genetic machinery for malignant progression. Indeed, hypoxia has been associated with metastasis, which usually leads to a very poor prognostic outcome (Rankin and Giaccia, 2016). Although metastasis accounts for the great majority of cancer-associated deaths, this complex process still remains the least understood aspect of cancer biology (Lambert et al., 2017). In this regard the prerequisites for the migration of tumor cells from a primary site to a secondary/metastatic site include weakening of the cell-to-cell adhesion and capability to directionally move away from the tumor mass toward an oxygenated blood vessel (Seyfried and Huysentruyt, 2013). While the molecular mechanisms responsible for the lessening of the intercellular cell adhesion have been largely ascertained, those enabling the directional “navigation” away from the mass have, only recently, started to be explored.

Besides bacteria (Taylor et al., 1999; Sporer et al., 2017), response to O₂ gradient has started only lately to be assessed in simple eukaryotic model systems (Gray et al., 2004; Chang et al., 2006; Kirkegaard et al., 2016; Demir et al., 2020) and more recently in mammalian cells (Deygas et al., 2018).

Early studies on *Dictyostelium* demonstrated that the cells responded by moving up the oxygen gradient, while late in development, the prestalk-prespore pattern can be oriented by the gradient (Sternfeld and Bonner, 1977; Sternfeld and David, 1981). Hence, we have attempted to quantitatively assess whether *Dictyostelium* cells can escape hypoxia moving along an oxygen gradient. Our findings indicate that, as in other organisms, *Dictyostelium* cells react to hypoxia in a time scale of 30–60 min. This implies the presence of a very efficient detection mechanism. Our current results do not allow to distinguish between positive (aero)taxis or negative chemotaxis because of accumulation of repellent/s. However, depletion of key nutrients can be excluded, as starving cells showed the



same behavior as growing cells. In this context, however, we can maintain that migration is the result of oxygen gradient as a phenomenon, without implying a mechanistic cause-effect.

The cells migrate following the gradient by adopting a peculiar arrangement, consisting of a peripheral structure (*corona*) characterized by contiguous cells exhibiting high speed and significant directionality toward a region of suitable oxygen level.

Interestingly, the cells that converge to form the *corona* are not the most external ones, which would be those closer to the region with high oxygen concentration. Instead, the local density maximum, which identifies the *corona*, forms within the colony radius. If the *corona* formation was simply caused by a critical hypoxic level, the migration would, in principle, start from the center of the colony, and all cells would move to escape the region of hypoxia, as long as the critical value does not lead to rounding of the cells. On the other hand, if the trigger was only the presence of an oxygen gradient, the migration would start earlier at the border of the colony, where we measured a slight oxygen gradient already 5 min after the confinement. A minimal model of this phenomenon (excluding intercellular communication) could consider as possible cause of the observed migration a critical hypoxic level in the presence of an oxygen gradient.

In contrast to *Dictyostelium* clusters, mammalian cell clusters under hypoxic conditions do not arrange so neatly, although a sort of “inner-core,” characterized by almost stationary cells, is common to both cell types (Deygas et al., 2018). The mechanism leading to this singular arrangement assumed by *Dictyostelium* cells remains currently unknown. Nevertheless, a detailed analysis of the dynamics of aerotaxis in *Dictyostelium* suggests that such arrangement is not random but that it is dictated by dynamic microenvironmental conditions. Behind the *corona*, displaying a rather high cellular density, we identified a wider region with lower density, in which the cells are appreciably elongated. Remarkably, the cells immediately behind the *corona* showed the highest speed, although their directionality was lower than that of the *corona*. We also noticed that, even if *Dictyostelium* WT cells are incubated in the axenic medium, after approximately 10–15 h, cell duplication is largely inhibited.

While drafting this manuscript, the team of Rieu reported results that mostly overlapped with ours (Cochet-Escartin et al., 2021). However, the experimental settings are quite different, and there are some contrasting results. For example, they suggest that, in growing cells, cell division plays an important role during aerotactic migration, while in our case, if any, this is restricted exclusively to the early-mid events. Noteworthy, our findings achieved by starving cells strengthen the hypothesis that, at least under our experimental settings, the role played by cell division is negligible for reacting to an oxygen gradient and for the *corona* formation and propagation.

Such discrepancy might be due to the different number of cells used for the spot assay to induce the oxygen gradient, giving rise to different microenvironmental conditions. Similarly, their experiments do not show radial motion of the cells outside the *corona*.

Overall, our analysis indicates that the aerotaxis migration differs from all the other *Dictyostelium* taxis (i.e., chemo-, electro- and rheo-taxis) so far described in the social amoeba (Zhao et al., 2002; Decave et al., 2003; Lima et al., 2014; Devreotes and Horwitz, 2015; Gao et al., 2015). We also assessed the migration behavior of developing cellular aggregates under confined conditions. Diversely from vegetative cells, aggregating cells have acquired different properties, such as the ability to produce and secrete the chemoattractant cAMP and to tightly adhere to each other by virtue of the adhesion molecule gp80/csA

(Noegel et al., 1985). Accordingly, *Dictyostelium* cell aggregates have recently been regarded as a potential and challenging model to investigate solid tumor mass (Trigos et al., 2018; Mathavarajah et al., 2021). Under hypoxic conditions, the aggregates became loose and portions of them detached within minutes. This finding suggests weakening of cell-cell adhesion. Even if different time scales and distinct molecular players are involved, such behavior recalls the epithelial-mesenchymal transition that is pivotal in favoring the metastasis process (Pastushenko and Blanpain, 2019). Our data indicate that, because of the short time window, the reduced cell-cell adhesion is independent from a transcriptional event, suggesting rapid regulation, internalization, or post-translational modification of the adhesion molecules. Furthermore, these findings definitely indicate that hypoxia-sensing mechanisms are present at both the vegetative and aggregation stages, suggesting a common sensor that is retained throughout *Dictyostelium* life cycle. This would be consistent with early reports that an oxygen gradient regulates aggregate size, migration, and pattern formation (Sternfeld and Bonner, 1977; Sternfeld and David, 1981) as well as gene expression (Schiavo and Bisson, 1989; Sandonà et al., 1995).

In animals, a crucial oxygen sensor is the transcription factor HIF1 α that under normoxic conditions has a very short half-life, while its degradation is retarded under decreasing oxygen concentration conditions. The more stable HIF1 α further translocates to the nucleus, where it dimerizes with HIF1 β , and the dimer eventually regulates gene transcription (Semenza, 2012). However, very recent data with animal cells (Kirkegaard et al., 2016; Deygas et al., 2018) indicate that HIF1 α does not act as a sensor for aerotaxis. The *Dictyostelium* genome does not encode for the putative HIF1 α . Interestingly, in mammalian cells incubated under hypoxic conditions, the driving event triggering the cell movement toward an oxygen source is intracellular accumulation, restricted to the very peripheral cells of the cluster, of hydrogen peroxide (Deygas et al., 2018). Hydrogen peroxide is a rather unstable molecule. However, it is more stable and less noxious than other reactive oxygen species (ROS), but interconvertible with other forms such as hydroxyl radicals and singlet oxygen by iron-catalyzed Haber-Weiss reactions. Like other cells, *Dictyostelium* amoebae dispose hydrogen peroxide with the enzyme catalase, degrading it to H₂O + O₂ (Parish, 1975; Hayashi and Suga, 1978; Sepasi Tehrani and Moosavi-Movahedi, 2018). The *Dictyostelium* genome harbors two catalase-encoding genes, *catA* and *catB*. Whereas the latter is prespore-specific, the former shows a fairly constant gene expression level at all stages of growth and development (Garcia et al., 2000; Garcia et al., 2002). Hence, we analyzed the aerotactic behavior of the *Dictyostelium catA*/null strain that, although aggregating and developing normally, reacted to oxygen deprivation faster than the WT strain. How can the suppression of catalase A affect cell migration? Hypoxia has been shown to favor the synthesis of plasmalogens, which occurs in peroxisomes (Jain et al., 2020). Their synthesis will increase the ratio of unsaturated vs. saturated phospholipids in the membrane, favoring membrane fluidity (Nagura et al., 2004; Dean and Lodhi, 2018), which in turn could result in increased cell motility (Tarabozetti et al., 1989; Edmond et al., 2015; Zhao et al., 2016; Angelucci et al., 2018).

We speculate that ROS accumulation, resulting from hypoxia, stimulates plasmalogen synthesis, a process further enhanced by catalase A inactivation. It is worth mentioning, in this context, that the plasmalogen form of phosphatidylethanolamine is the major phospholipid constituent of *Dictyostelium* cell membrane (Weeks and Herring, 1980). In addition, hydrogen peroxide is also a crucial regulator of the cytoskeleton dynamics on the leading edge of migrating cells and thus controlling cell polarity (Hurd et al., 2012; Emre et al., 2021).

Overall, these results let hypothesize that catalase, by regulating intracellular hydrogen peroxide pool, represents a component or regulator of a putative sensor machinery plausibly conserved throughout different kingdoms.

In an attempt to identify other possible players regulating aerotaxis, we tested a panel of mutants defective in chemotaxis. In terms of signal transduction mechanisms, *Dictyostelium* chemotaxis and electrotaxis diverge relatively little (e.g., G-protein and PKBR-1), while most of the players appear to be shared (pianissimo, rip3, and PTEN, etc.). Because we were unable to examine the whole collection of chemo- and electro-taxis mutants, we chose several archetypal strains and analyzed their behavior. *Dictyostelium* cells possess only one G β subunit, which is essential for all G protein-dependent signal transduction pathways. Unlike chemotaxis, but more similar to electrotaxis, the G protein appears to be a secondary regulator constraining the bias shown by our survey carried out with the G β^{null} mutant. Likewise, our findings indicate that *Dictyostelium* hypoxia-driven migration is a process independent from mTORC2 that is, on the contrary, an essential regulator for both chemo- and electro-taxis (Chen et al., 1997; Pergolizzi et al., 2002; Lee et al., 2005; Gao et al., 2015). Lastly, our evidence suggests that, different from electrotaxis, PKBR-1 acts as a negative regulator during the aerotactic *corona* migration. The different aerotaxis behavior between the *pkbR1^{null}* and mTORC2-deficient mutants is puzzling. Besides its mTORC2 independent activation, the molecular mechanisms by which PKBR-1 negatively regulates the *corona* speed remain currently unknown. PKB activation is rather complex, and its full activation is achieved only when both the activation loop (AL) and hydrophobic motif (HM) are phosphorylated (Pearce et al., 2010). However, partial PKB activation can be attained in an mTORC2-independent way through sole AL phosphorylation (Guertin et al., 2006). Strikingly, the role of PKBR-1 seems to be strictly restricted in controlling the velocity of *corona* migration.

Although the signaling that finely tunes the response to oxygen deprivation in *Dictyostelium* remains mostly unknown, based on our discoveries, we can speculate on a possible model that could be tested in future experiments 1 (Figure 8). In analogy with

mammalian cells, this model proposes that a *Dictyostelium* cell cluster responds to oxygen depletion through a peripheral cell sub-population. This very early event is most likely triggered by an intracellular accumulation of H₂O₂ without the involvement of substantial transcriptional events. Afterward, the cell cluster arranges with a peripheral ring structure, the *corona*, that moves outward and whose speed is negatively regulated by PKBR-1.

In conclusion *Dictyostelium*, represents a novel alternative and genetically amenable model that can be widely exploited to unravel some basic cell biology aspects of directional migration toward oxygen.

DATA AVAILABILITY STATEMENT

The original contributions presented in the study are included in the article/**Supplementary Material**, further inquiries can be directed to the corresponding author.

AUTHOR CONTRIBUTIONS

BP, EB, MO, and MB contributed to the conception and design of the study. BP, EB, CP, and SA conducted the experiments. MB and MO developed the analytic tools and analyzed the data. BP, EB, MO, and MB wrote the first draft of the manuscript. SB revised the manuscript and contributed to the discussion. All authors contributed to manuscript revision, and read and approved the submitted version.

FUNDING

This study was supported by a grant of AIRBB to BP and the “Departments of Excellence” grant of the MIUR (L. 232/2016) to MO and MB.

ACKNOWLEDGMENTS

We thank Guido Serini for the helpful discussions.

SUPPLEMENTARY MATERIAL

The Supplementary Material for this article can be found online at: <https://www.frontiersin.org/articles/10.3389/fcell.2021.720623/full#supplementary-material>

REFERENCES

- Allan, D. B., Caswell, T., Keim, N. C., van der Wel, C. M., and Verweij, R. W. (2021). *soft-matter/trackpy: Trackpy v0.5.0*. Genève: Zenodo.
- Angelucci, C., D'Alessio, A., Iacopino, F., Proietti, G., Di Leone, A., Masetti, R., et al. (2018). Pivotal role of human stearoyl-CoA desaturases (SCD1 and 5) in breast cancer progression: oleic acid-based effect of SCD1 on cell migration and a novel pro-cell survival role for SCD5. *Oncotarget* 9, 24364–24380. doi: 10.18632/oncotarget.25273
- Ashworth, J. M., and Watts, D. J. (1970). Metabolism of the cellular slime mould *Dictyostelium discoideum* grown in axenic culture. *Biochem. J.* 119, 175–182. doi: 10.1042/bj1190175
- Bozzaro, S. (2013). The model organism *dictyostelium discoideum*. *Methods Mol. Biol.* 983, 17–37. doi: 10.1007/978-1-62703-302-2_2
- Bozzaro, S. (2019). The past, present and future of *Dictyostelium* as a model system. *Int. J. Dev. Biol.* 63, 321–331. doi: 10.1387/ijdb.190128sb
- Bozzaro, S., Hagmann, J., Noegel, A., Westphal, M., Calautti, E., and Bogliolo, E. (1987). Cell differentiation in the absence of intracellular and extracellular

- cyclic AMP pulses in *Dictyostelium discoideum*. *Dev. Biol.* 123, 540–548. doi: 10.1016/0012-1606(87)90412-x
- Bradski, G. (2000). The Opencv library. *Dr. Dobbs J. Software Tools* 120, 122–125. doi: 10.1109/MRA.2009.933612
- Chang, A. J., Chronis, N., Karow, D. S., Marletta, M. A., and Bargmann, C. I. (2006). A distributed chemosensory circuit for oxygen preference in *C. elegans*. *PLoS Biol.* 4:e274. doi: 10.1371/journal.pbio.0040274
- Chen, M. Y., Long, Y., and Devreotes, P. N. (1997). A novel cytosolic regulator, Pianissimo, is required for chemoattractant receptor and G protein-mediated activation of the 12 transmembrane domain adenylyl cyclase in *Dictyostelium*. *Genes Dev.* 11, 3218–3231. doi: 10.1101/gad.11.23.3218
- Claesson-Welsh, L. (2020) Oxygen sensing; a stunningly elegant molecular machinery hijacked in cancer. *Ups J Med Sci.* 125, 205–210. doi: 10.1080/03009734.2020.1769231
- Cochet-Escartin, O., Mete, D., Satomi, H., Blandine, A., Philippe, G., Mikaelian, I., et al. (2021). Hypoxia triggers collective aerotactic migration in *Dictyostelium discoideum*. *eLife* 10:e64731. doi: 10.7554/eLife.64731
- Dean, J. M., and Lodhi, I. J. (2018). Structural and functional roles of ether lipids. *Protein Cell* 9, 196–206. doi: 10.1007/s13238-017-0423-425
- Decave, E., Rieu, D., Dalous, J., Fache, S., Brechet, Y., Fourcade, B., et al. (2003). Shear flow-induced motility of *Dictyostelium discoideum* cells on solid substrate. *J. Cell Sci.* 116, 4331–4343. doi: 10.1242/jcs.00726
- Demir, E., Yaman, Y. I., Basaran, M., and Kocabas, A. (2020). Dynamics of pattern formation and emergence of swarming in *Caenorhabditis elegans*. *eLife* 9:e52781. doi: 10.7554/eLife.52781
- Devreotes, P., and Horwitz, A. R. (2015). Signaling networks that regulate cell migration. *Cold Spring Harb. Perspect. Biol.* 7:a005959. doi: 10.1101/cshperspect.a005959
- Deygas, M., Gadet, R., Gillet, G., Rimokh, R., Gonzalo, P., and Mikaelian, I. (2018). Redox regulation of EGFR steers migration of hypoxic mammary cells towards oxygen. *Nat. Commun.* 9:4545. doi: 10.1038/s41467-018-06988-6983
- Dunwoodie, S. L. (2009). The role of hypoxia in development of the Mammalian embryo. *Dev. Cell* 17, 755–773. doi: 10.1016/j.devcel.2009.11.008
- Edmond, V., Dufour, F., Poiroux, G., Shoji, K., Malleter, M., Fouqué, A., et al. (2015). Downregulation of ceramide synthase-6 during epithelial-to-mesenchymal transition reduces plasma membrane fluidity and cancer cell motility. *Oncogene* 34, 996–1005. doi: 10.1038/ncr.2014.55
- Emre, B., Johanna, K., and Yvonne, S. (2021). Redox Regulation of the actin cytoskeleton in cell migration and adhesion: on the way to a spatiotemporal view. *Front Cell Dev. Biol.* 8. doi: 10.3389/fcell.2020.618261
- Fey, P., Dodson, R. J., Basu, S., Hartline, E. C., and Chisholm, R. L. (2019). dictyBase and the Dicty Stock Center (version 2.0) - a progress report. *Int. J. Dev. Biol.* 63, 563–572. doi: 10.1387/ijdb.190226pf
- Fisher, P. R., and Annesley, S. J. (2006). Slug phototaxis, thermotaxis, and spontaneous turning behavior. *Meth. Mol. Biol.* 346, 137–170.
- Gao, R., Zhao, S., Jiang, X., Sun, Y., Zhao, S., Gao, J., et al. (2015). A large-scale screen reveals genes that mediate electrotaxis in *Dictyostelium discoideum*. *Sci. Signal.* 8:ra50. doi: 10.1126/scisignal.aab0562
- Garcia, M. X. U., Foote, C., van Es, S., Devreotes, P. N., Alexander, S., and Alexander, H. (2000). Differential developmental expression and cell type specificity of *Dictyostelium* catalases and their response to oxidative stress and UV-light. *Biochim. Biophys. Acta* 1492, 295–310. doi: 10.1016/s0167-4781(00)00063-4
- Garcia, M. X. U., Roberts, C., Alexander, H., Stewart, A. M., Harwood, A., Alexander, S., et al. (2002). Methanol and acriflavine resistance in *Dictyostelium* are caused by loss of catalase. *Microbiology* 148, 333–340. doi: 10.1099/00221287-148-1-333
- Gray, J. M., Karow, D. S., Lu, H., Chang, A. J., Chang, J. S., Ellis, R. E., et al. (2004). Oxygen sensation and social feeding mediated by a *C. elegans* guanylate cyclase homologue. *Nature* 430, 317–322. doi: 10.1038/nature02714
- Guertin, D. A., Stevens, D. M., Thoreen, C. C., Burds, A. A., Kalaany, N. Y., Moffat, J., et al. (2006). Ablation in mice of the mTORC components raptor, rictor, or mLST8 reveals that mTORC2 is required for signaling to Akt-FOXO and PKCalpha, but not S6K1. *Dev. Cell* 11, 859–871. doi: 10.1016/j.devcel.2006.10.007
- Guido, I., Diehl, D., Olszok, N. A., and Bodenschatz, E. (2020). Cellular velocity, electrical persistence and sensing in developed and vegetative cells during electrotaxis. *PLoS One* 15:e0239379. doi: 10.1371/journal.pone.0239379
- Hayashi, H., and Suga, T. (1978). Some characteristics of peroxisomes in the slime mold, *Dictyostelium discoideum*. *J. Biochem.* 84, 513–520. doi: 10.1093/oxfordjournals.jbchem.a132155
- Horsman, M. R., and Overgaard, J. (2016). The impact of hypoxia and its modification of the outcome of radiotherapy. *J. Radiat. Res.* 57, 90–98. doi: 10.1093/jrr/rrw007
- Hurd, T. R., DeGennaro, M., and Lehmann, R. (2012). Redox regulation of cell migration and adhesion. *Trends Cell Biol.* 22, 107–115. doi: 10.1016/j.tcb.2011.11.002
- Jain, I. H., Calvo, S. E., Markhard, A. L., Skinner, O. S., To, T. L., Ast, T., et al. (2020). Genetic screen for cell fitness in high or low oxygen highlights mitochondrial and lipid metabolism. *Cell* 181, 716–727.e11. doi: 10.1016/j.cell.2020.03.029
- Jeon, T. J., Gao, R., Kim, H., Lee, A., Jeon, P., Devreotes, P. N., et al. (2019). Cell migration directionality and speed are independently regulated by RasG and Gβ in *Dictyostelium* cells in electrotaxis. *Biol. Open* 8:bio042457. doi: 10.1242/bio.042457
- Kirkegaard, J. B., Bouillant, A., Marron, A. O., Leptos, K. C., and Goldstein, R. E. (2016). Aerotaxis in the closest relatives of animals. *eLife* 5:e18109. doi: 10.7554/eLife.18109
- Lambert, A. W., Pattabiraman, D. R., and Weinberg, R. A. (2017). Emerging biological principles of metastasis. *Cell* 168, 670–691. doi: 10.1016/j.cell.2016.11.037
- Lee, S., Comer, F. I., Sasaki, A., McLeod, I. X., Duong, Y., Okumura, K., et al. (2005). TOR complex 2 integrates cell movement during chemotaxis and signal relay in *Dictyostelium*. *Mol. Biol. Cell* 16, 4572–4583. doi: 10.1091/mbc.e05-04-0342
- Lewis, D. M., Park, K. M., Tang, V., Xu, Y., Pak, K., and Eisinger-Mathason, T. S. E. A. (2016). Intratumoral oxygen gradients mediate sarcoma cell invasion. *Proc. Natl. Acad. Sci. U S A.* 113, 9292–9297. doi: 10.1073/pnas.1605317113
- Lilly, P., Wu, L. J., Welker, D. L., and Devreotes, P. N. (1993). A G-protein beta-subunit is essential for *Dictyostelium* development. *Genes Dev.* 7, 986–995. doi: 10.1101/gad.7.6.986
- Lima, W. C., Vinet, A., Pieters, J., and Cosson, P. (2014). Role of PKD2 in rheotaxis in *Dictyostelium*. *PLoS One* 9:e88682. doi: 10.1371/journal.pone.0088682
- Mathavarajah, S., VanInderstine, C., Dellaire, G., and Huber, R. J. (2021). Cancer and the breakdown of multicellularity: what *Dictyostelium discoideum*, a social amoeba, can teach us. *Bioessays* 43:e2000156. doi: 10.1002/bies.202000156
- Meili, R., Ellsworth, C., and Firtel, R. A. (2000). A novel Akt/PKB-related kinase is essential for morphogenesis in *Dictyostelium*. *Curr. Biol.* 10, 708–717. doi: 10.1016/s0960-9822(00)00536-4
- Muz, B., de la Puente, P., Azab, F., and Azab, A. K. (2015). The role of hypoxia in cancer progression, angiogenesis, metastasis, and resistance to therapy. *Hypoxia (Auckl)* 3, 83–92. doi: 10.2147/hp.s93413
- Nagura, M., Saito, M., Iwamori, M., Sakakihara, Y., and Igarashi, T. (2004). Alterations of fatty acid metabolism and membrane fluidity in peroxisome-defective mutant ZP102 cells. *Lipids* 39, 43–50. doi: 10.1007/s11745-004-1200-z
- Noegel, A., Harloff, C., Hirth, P., Merkl, R., Modersitzki, M., Stadler, J., et al. (1985). Probing an adhesion mutant of *Dictyostelium discoideum* with cDNA clones and monoclonal antibodies indicates a specific defect in the contact site A glycoprotein. *EMBO J.* 4, 3805–3810
- Pal, D. S., Li, X., Banerjee, T., Miao, Y., and Devreotes, P. N. (2019). The excitable signal transduction networks: movers and shapers of eukaryotic cell migration. *Int. J. Dev. Biol.* 63, 407–416. doi: 10.1387/ijdb.190265pd
- Parish, R. W. (1975). Mitochondria and peroxisomes from the cellular slime mould *Dictyostelium discoideum*. Isolation techniques and urate oxidase association with peroxisomes. *Eur. J. Biochem.* 58, 523–531. doi: 10.1111/j.1432-1033.1975.tb02401.x
- Parks, S. K., Cormerais, Y., and Pouyssegur, J. (2017). Hypoxia and cellular metabolism in tumour pathophysiology. *J. Physiol.* 595, 2439–2450. doi: 10.1113/jp273309
- Pastushenko, I., and Blanpain, C. (2019). EMT transition states during tumor progression and metastasis. *Trends Cell Biol.* 29, 212–226. doi: 10.1016/j.tcb.2018.12.001
- Pearce, L. R., Komander, D., and Alessi, D. R. (2010). The nuts and bolts of AGC protein kinases. *Nat. Rev. Mol. Cell Biol.* 11, 9–22. doi: 10.1038/nrm2822
- Pergolizzi, B., Bozzaro, S., and Bracco, E. (2017a). G-Protein dependent signal transduction and ubiquitination in *Dictyostelium*. *Int. J. Mol. Sci.* 18:2180. doi: 10.3390/ijms18102180

- Pergolizzi, B., Bracco, E., and Bozzaro, S. (2017b). A new HECT ubiquitin ligase regulating chemotaxis and development in *Dictyostelium discoideum*. *J. Cell Sci.* 130, 551–562. doi: 10.1242/jcs.194225
- Pergolizzi, B., Peracino, B., Silverman, J., Ceccarelli, A., Noegel, A., Devreotes, P., et al. (2002). Temperature-sensitive inhibition of development in *Dictyostelium* due to a point mutation in the *piaA* gene. *Dev. Biol.* 251, 18–26. doi: 10.1006/dbio.2002.0809
- Rankin, E. B., and Giaccia, A. J. (2016). Hypoxic control of metastasis. *Science* 352, 175–180. doi: 10.1126/science.aaf4405
- Rey, S., and Semenza, G. L. (2010). Hypoxia-inducible factor-1-dependent mechanisms of vascularization and vascular remodeling. *Cardiovasc. Res.* 1, 236–242. doi: 10.1093/cvr/cvq045
- Sandonà, D., Gastaldello, S., Rizzuto, R., and Bisson, R. (1995). Expression of cytochrome c oxidase during growth and development of *Dictyostelium*. *J. Biol. Chem.* 270, 5587–5593. doi: 10.1074/jbc.270.10.5587
- Schiavo, G., and Bisson, R. (1989). Oxygen influences the subunit structure of cytochrome c oxidase in the slime mold *Dictyostelium discoideum*. *J. Biol. Chem.* 264, 7129–7134. doi: 10.1016/s0021-9258(18)83211-2
- Semenza, G. L. (2012). Hypoxia-inducible factors in physiology and medicine. *Cell* 148, 399–408. doi: 10.1016/j.cell.2012.01.021
- Sepasi Tehrani, H., and Moosavi-Movahedi, A. A. (2018). Catalase and its mysteries. *Prog. Biophys. Mol. Biol.* 140, 5–12. doi: 10.1016/j.pbiomolbio.2018.03.001
- Seyfried, T. N., and Huysentruyt, L. C. (2013). On the origin of cancer metastasis. *Crit. Rev. Oncog.* 18, 43–73. doi: 10.1615/critrevoncog.v18.i1-2.40
- Sporer, A. J., Kahl, L. J., Price-Whelan, A., and Dietrich, L. E. P. (2017). Redox-Based regulation of bacterial development and behavior. *Annu. Rev. Biochem.* 86, 777–797. doi: 10.1146/annurev-biochem-061516-44453
- Sternfeld, J., and Bonner, J. T. (1977). Cell differentiation in *Dictyostelium* under submerged conditions. *Proc. Natl. Acad. Sci. U S A.* 74, 268–271. doi: 10.1073/pnas.74.1.268
- Sternfeld, J., and David, C. N. (1981). Oxygen gradients cause pattern orientation in *Dictyostelium* cell clumps. *J. Cell Sci.* 50, 9–17.
- Stuelten, C. H., Parent, C. A., and Montell, D. J. (2018). Cell motility in cancer invasion and metastasis: insights from simple model organisms. *Nat. Rev. Cancer* 18, 296–312. doi: 10.1038/nrc.2018.15
- Taraboletti, G., Perin, L., Bottazzi, B., Mantovani, A., Giavazzi, R., and Salmons, M. (1989). Membrane fluidity affects tumor-cell motility, invasion and lung-colonizing potential. *Int. J. Cancer* 44, 707–713. doi: 10.1002/ijc.2910440426
- Taylor, B. L., Zhulin, I. B., and Johnson, M. S. (1999). Aerotaxis and other energy-sensing behavior in bacteria. *Annu. Rev. Microbiol.* 53, 103–128. doi: 10.1146/annurev.micro.53.1.103
- Trigos, A. S., Pearson, R. B., Papenfuss, A. T., and Goode, D. L. (2018). How the evolution of multicellularity set the stage for cancer. *Br. J. Cancer* 118, 145–152. doi: 10.1038/bjc.2017.398
- Weeks, G., and Herring, F. G. (1980). The lipid composition and membrane fluidity of *Dictyostelium discoideum* plasma membranes at various stages during differentiation. *J. Lipid. Res.* 21, 681–686.
- Wilson, D. F. (2017). Oxidative phosphorylation: regulation and role in cellular and tissue metabolism. *J. Physiol.* 595, 7023–7038. doi: 10.1113/jp273839
- Zhao, M., Jin, T., McCaig, C. D., Forrester, J. V., and Devreotes, P. N. (2002). Genetic analysis of the role of G protein-coupled receptor signaling in electro taxis. *J. Cell Biol.* 157, 921–927. doi: 10.1083/jcb.200112070
- Zhao, W., Prijic, S., Urban, B. C., Tisza, M. J., Zuo, Y., Li, L., et al. (2016). Candidate antimetastasis drugs suppress the metastatic capacity of breast cancer cells by reducing membrane fluidity. *Cancer Res.* 76, 2037–2049. doi: 10.1158/0008-5472.can-15-1970

Conflict of Interest: The authors declare that the research was conducted in the absence of any commercial or financial relationships that could be construed as a potential conflict of interest.

Publisher's Note: All claims expressed in this article are solely those of the authors and do not necessarily represent those of their affiliated organizations, or those of the publisher, the editors and the reviewers. Any product that may be evaluated in this article, or claim that may be made by its manufacturer, is not guaranteed or endorsed by the publisher.

Copyright © 2021 Biondo, Panuzzo, Ali, Bozzaro, Osella, Bracco and Pergolizzi. This is an open-access article distributed under the terms of the Creative Commons Attribution License (CC BY). The use, distribution or reproduction in other forums is permitted, provided the original author(s) and the copyright owner(s) are credited and that the original publication in this journal is cited, in accordance with accepted academic practice. No use, distribution or reproduction is permitted which does not comply with these terms.